

MUON BEAMS AT THE LAMPF BIOMEDICAL CHANNEL

M.A. Paciotti, J.N. Bradbury, and O.M. Rivera
 Los Alamos National Laboratory
 Los Alamos, New Mexico 87545*

Summary

Modifications have been made to the LAMPF biomedical channel that allow the delivery of intense muon beams for physics experiments while retaining the design high-flux pion capability. Two types of muon beams have been developed: first, muons from the backward decay of pions and second, "cloud" muons, from the target region, momentum-degraded in the channel to reduce the pion component. Muons are collected from a region between the second and third bending magnets in the channel which can contain a Be degrader. A momentum-dispersed image is formed at a new downstream slit which is used to determine the momentum spread of both types of muon beams. The decay beam provides good polarization and low electron contamination. The degraded beam has higher intensity but about 40% electron contamination. Both beams have a pion contamination of about 3%.

Introduction

Hardware and tuning techniques are available to make particle delivery channels rather versatile in terms of beam composition and parameters. Magnetic channels can be designed or modified to permit the delivery of several types of particles with a range of values for momentum, momentum spread, beam purity, and flux. Codes such as TRANSPORT¹ and TURTLE² may be used to study the effects of varying the fields of magnets and of adding hardware such as momentum degraders and slit systems. This paper describes the results of a program aimed at obtaining useful muon beams from a channel designed to deliver a high flux of pions.

Description of Channel Configuration for Muon Tunes

Two types of muon tunes have been recently developed for the LAMPF biomedical channel. The first type utilizes the very intense source of "cloud" muons produced near the target region; typical beams with the channel tuned for pions have a 15% component of cloud muons.³ The first section of the channel focuses a dispersed beam at the location of the wedge degrader indicated in Figure 1.⁴ The wedge is replaced by a uniform thickness Be degrader which provides momentum separation between pions and cloud muons. An analyzer section consisting of elements B3 and Q4 is used to regain good momentum resolution and achieve particle separation. A momentum dispersed image of slit S2, directly following the degrader, is formed between Q4 and Q5. An additional slit assembly S3 is installed at this second bend-plane focus to select the momentum bite of the analyzer. Wire chambers before and after B3 are used routinely to measure particle momenta. This system was employed in Q4 optimization and gave an analyzer FWHM momentum resolution of 2.8% for 83 MeV/c muons.

A second tune type is the backward-decay configuration that collects muons from pion decays in the region between B2 and B3 without the degrader

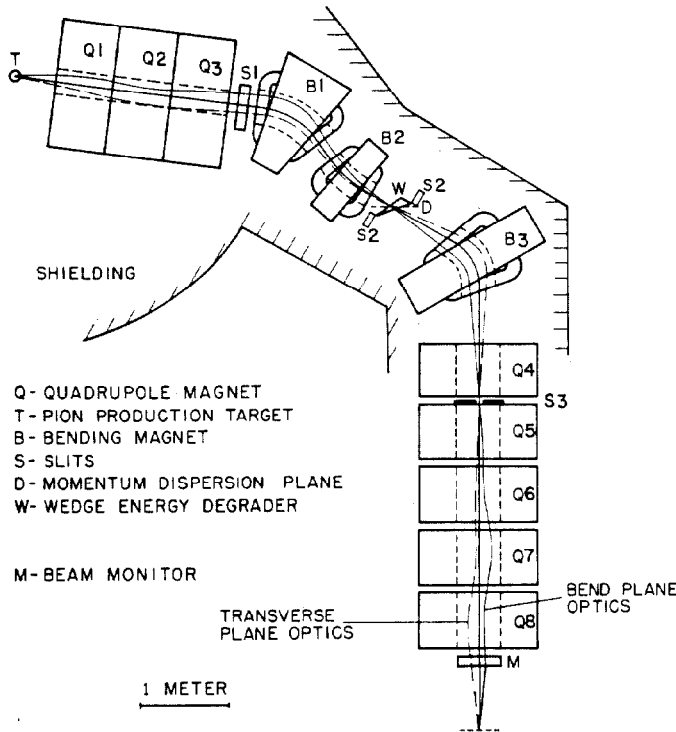


Fig. 1. LAMPF biomedical channel modified for muon beam capability with addition of slit S3 located at dispersed image of S2.

present. The slit S2 limits the source size for the analyzer, for both the backward decay and the degraded cloud muon tunes. Electrons and pions are easily removed by the analyzer, resulting in clean muon beams that are expected to have good polarization.

Cloud Muon Tunes

The cloud beam is degraded in momentum in order to eliminate pion contamination and to obtain smaller momentum spread, smaller spot size, and higher rate than is possible for decay tunes. The effect of the degrader on the particles, identified by pulse height in a thin scintillator, is illustrated in Figure 2. The analyzer and beam-shaping section of the channel are fixed at 83 MeV/c while the momentum of the first section is varied. The normal setting for the first section is 123 MeV/c at the muon peak. The large differences in dE/dx between particles result in substantial differences in momentum after the degrader. Pions are very well separated from muons at the muon peak. Electrons are present, however, at all momenta due to large radiative energy losses.

*Work performed under the auspices of the U.S. Department of Energy

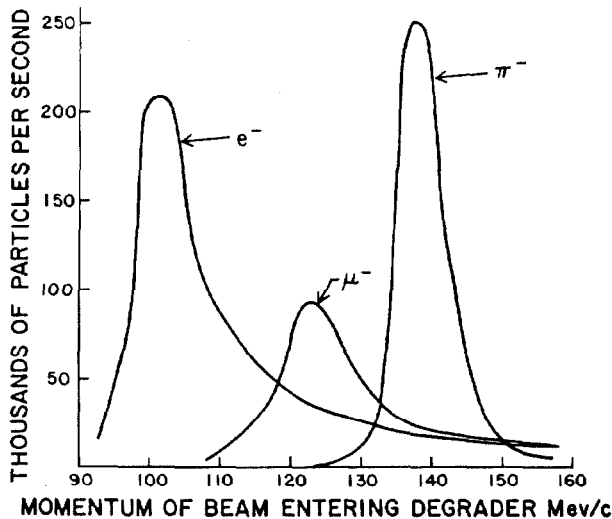


Fig. 2. Function of Be degrader. π , μ , and e are detected with analyzer set to 83 MeV/c. The central momentum of the composite beam entering the degrader is swept by varying Q1-B2. Rates are measured with a 1.3 g/cm² target which is 1/7 of the normal production target thickness. This "thin" target reduces electron production in the target by a factor of 2 from the normal target.⁵

The relative heights of the peaks are strongly affected by scattering in the degrader. The approximate composition before the degrader is 20% μ^- , 20% e^- , and 60% π^- . The electrons suffer the least scattering and after the degrader are about equal in rate to pions, many of which have been scattered out of the acceptance of the analyzer. Another effect reducing the muon intensity arises from the fact that the particles are already momentum analyzed entering the degrader as it is coincident with the focal plane of the first section. The muons have considerably poorer momentum resolution at this point since they arise from an extended source; hence the capture efficiency of the analyzer is lower.

Electron Contamination In Cloud Tunes

The degrader thickness used was the minimum that eliminated nearly all pions on the basis of TURTLE calculations. The large fraction of surviving electrons observed was surprising since the electron collision energy loss is much smaller than muon energy loss in the degrader and e^- and cloud μ^- are incident on the degrader in about equal numbers.

As revealed by Figure 2, the biggest factor in enhancing e^- relative to μ^- is the reduction of μ^- by scattering out of the analyzer acceptance. In addition, a study of the effects of electron radiative losses was undertaken. Electrons with a momentum of 123 MeV/c (the first-section momentum used for muon tunes) were delivered to the 5.4 cm Be degrader. The radiative tail was observed experimentally by sweeping the momentum of the analyzer and recording electron transmission, producing the curve in Fig. 3. The properties of this incident electron beam were taken from measurements with the B3 wire chambers without the degrader present. The calculated curve comes from the Electron-Gamma Shower code EGS⁶. An angular cut was

applied to e^- exiting the degrader corresponding to the acceptance of the analyzer. The two curves are normalized by numbers of particles so that the comparison in the tail is not distorted by the non-equality of the spreads in the peak regions. Lack of agreement in the peaks is attributed to imperfect knowledge of the momentum spread of the beam for the specific slit apertures used.

The good match in the tail region indicates that the electron component at the muon momentum of 83 MeV/c arises from radiative energy loss. This calculation also predicts correctly the 30% reduction in electron component observed using Al instead of Be as a degrader material with the same muon energy loss.

Beam Properties

Table I contains beam properties for decay and cloud tunes and includes for comparative purposes data for two high-flux pion tunes designed for patient dynamic treatment.

The decay and cloud tunes are listed in order of increasing slit aperture. The bend-plane rms spot size (σ_x) increases as the source size at S3 becomes larger. The channel contains He bags with air gaps for slits and wire chambers, but beams with momenta as low as 65 MeV/c still have acceptable spot size and momentum spread.

Table I also contains the rms momentum spreads for muon beams as a range width (σ_z) measured in water. Somewhat smaller momentum spreads are measured with the B3 wire chambers. For example, using small slit apertures, a cloud tune has σ_z of 1.2% whereas the range curve corresponds to σ_z of 1.8% after unfolding straggling. The TURTLE calculation including scattering predicted a momentum spread of 1.1%.

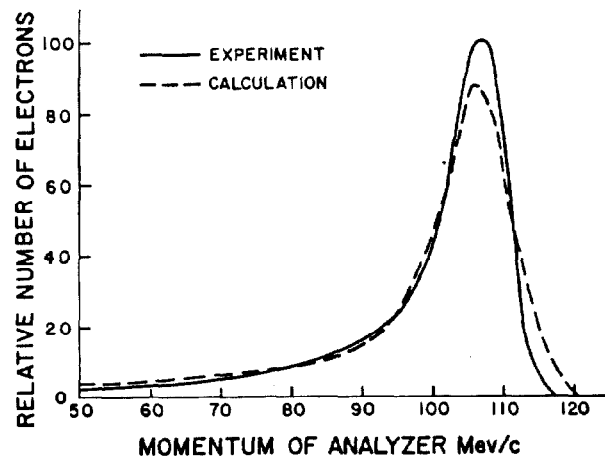


Fig. 3. Calculated and measured radiative electron tail for 123 MeV/c e^- incident on 5.4 cm Be degrader. The EGS code was used to calculate the spectrum with a limiting cut on angle to match analyzer acceptance.

Table I. Characteristics of Representative Beams.

Beam Type	Size in Air (cm)		Momentum Spread		Particles per Second $\times 10^{-6}$	Composition (%)			
	σ_x	σ_y	Range Width in Water σ_z (cm)			$e/e + \mu$	π/μ	μ/π	e/π
				σ_z (%)					
π^- 150 MeV/c	3.1	3.3		2.2	5.0×10^2		15	14	
π^- 190 MeV/c	3.2	3.2		1.8	7.5×10^2		12	7	
μ^- (backward decay)	2.3	3.0	0.32		0.26	3.7	2.0		
83 MeV/c	2.7	3.1	0.47		1.0				
	4.4	3.3	0.59		2.9				
μ^- (cloud using degrader and magnetic separation)	2.1	2.7	0.33		0.5	37	2.5		
83 MeV/c	2.6	2.7	0.39		1.8	37			
	3.6	2.9	0.44		3.6	37			

Notes:

1. Rates for positive particles are approximately 5 times those for negative particles.
2. Rates are for 500- μ A proton current on an A-5 target of 8.8 g/cm² pyrocarbon.
3. All distributions are Gaussian except decay beam momentum distribution, which has a high-momentum tail.
4. Cloud beams use a 5.4-cm beryllium degrader at the channel first focus.

Polarization of Backward Decay Beams

Polarization calculations were made for backward-decay beams with TURTLE modified to include calculation of the initial polarization of muons. Possible depolarization in the transport process through the magnets was not considered. Usually the polarization of backward-decay muon beams is high; however the source of particles in this channel is not ideal since the decay region is partly contained within the analyzer. The field in B3 is set for backward decay muons; the pions then follow a path of large radius. Decay muons traveling toward the inside of the arc can be accepted by the system and have low polarization. As the analyzer cannot reject these high momentum particles, the average polarization is reduced.

The calculations yield average polarizations from 83% to 88% for the tunes in Table I. The lowest rate tune has the smallest slit apertures, the smallest momentum spread, and therefore the best polarization. The calculations also predict that improvement in polarization can be obtained through collimation of the output beams where the higher momentum particles are not well focused.

The extensive measurements available for beam properties at the first focus allowed accurate prediction of decay beam rates and momentum spread. Measured spot sizes were, however, 30% larger than predicted.

Electron and Pion Beams

The data in Figure 2 suggest the use of the degrader for delivery of electron and pion beams with the same optics as the muons beams. The electron beam so produced is nearly pure (97% by the time-of-flight method) and has been valuable as a test beam for experiments requiring electron detectors.

The pion peak shown in Figure 2 has 19% ($\mu + e$) contamination and about three times the cloud muon rates quoted in Table I. Some stopping pion experiments cannot tolerate the direct high-intensity pion beam and, to suppress background, the smaller range spread available from an 80-MeV/c beam with a

narrow momentum bite is preferred. Since the optics is the same for each particle beam, the spot sizes and momentum spreads are similar to the cloud muon beam parameters listed in Table I.

References

1. Brown, K.L., Rothacker, F., Carey, D.C. and Iselin, Ch., SLAC-91 Rev. 1 (1974).
2. Brown, K.L. and Iselin, Ch.: DECAY TURTLE (Trace Unlimited Rays Through Lumped Elements), A computer program for simulating charged particle beam transport systems, including decay calculations. CERN 74-2, 5 February 1974.
3. Paciotti, M., Bradbury, J., Inoue, H., Rivera, O., and Sandford, S.: Beam Characteristics in the LAMPF Biomedical Channel, IEEE Trans. on Nucl. Sci. NS-28: 3150, 1981.
4. Paciotti, M.A., Bradbury, J.N., Helland, J.A., Hutson, R.L., Knapp, E.A., Rivera, O.M., Knowles, H.B., and Pfeuffer, G.: Tuning of the First Section of the Biomedical Channel at LAMPF. IEEE Trans. on Nucl. Sci. NS-22: 1784, 1975.
5. Paciotti, M., Amols, H., Bradbury, J., Rivera, O., Hogstrom, K., Smith, A., Inoue, H., Laubacher, D., and Sandford, S.: Pion Beam Development for the LAMPF Biomedical Project. IEEE Trans. on Nucl. Sci. NS-26 3071-3073, 1979.
6. Ford, R.L. and Nelson, W.R.: The EGS Code System: Computer Programs for the Monte Carlo Simulation of Electromagnetic Cascade Showers (Version 3). SLAC-210, UC-32, 1978.